

Analysis, Testing and Initial Recommendations on Collapse Limit States of Frames

by *Darren Vian, Mettupalayam Sivaselvan, Michel Bruneau and Andrei Reinhorn*

Research Objectives

The objective of this study is to develop a set of guidelines and analytical tools for use by practicing engineers to determine the collapse limit state of structures. A program of shake table testing of simple frames through collapse was carried out, and analytical strategies to capture this behavior have been developed and made available on the web via MCEER's users network. The research performed here helps to develop a better understanding of the collapse mechanism and provides tools for further investigation.

As inelastic behavior is more extensively relied upon in the dissipation of seismic input energy, the destabilizing effect of gravity becomes more significant in the structural evaluation of existing structures. However, practicing engineers have limited confidence in the adequacy of currently available analytical tools to accurately predict when collapse will occur (i.e., the collapse limit state). As a result, there is a need to investigate the seismic behavior of structures to enhance our understanding of the condition ultimately leading to their collapse, and to ensure public safety during extreme events. While many experimental studies and theoretical damage models support these calculated values, it remains that few experimental studies have pushed the shake table tests up to collapse.

This paper presents the results of research to provide some of that data through a program of shake-table testing of simple frames through collapse, developments of analytical strategies to capture this behavior, and recommendations for design. Note that every effort was made to ensure that the experimental data is fully documented (geometry, material properties, initial imperfections, detailed test results, etc.); it will be made broadly available on MCEER's Users Network such that these tests can be used at a later time by other researchers as a benchmark to which analytical models can be compared. An example of such use is the development made by the authors, described herein, using the benchmark test results.

Experimental Program

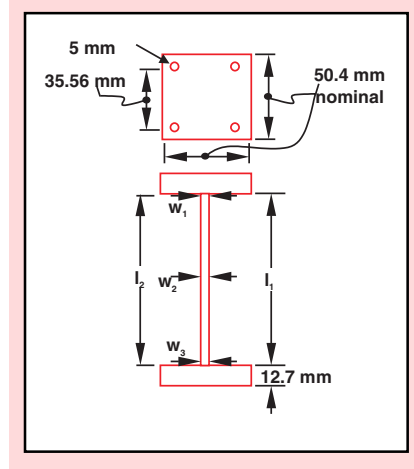
Fifteen specimens, each consisting of four columns, were tested to failure in the course of this research. These were subdivided into three groups of five with slenderness ratios of 100, 150, and 200. The dimen-

Sponsors

*National Science Foundation,
Earthquake Engineering
Research Centers Program*

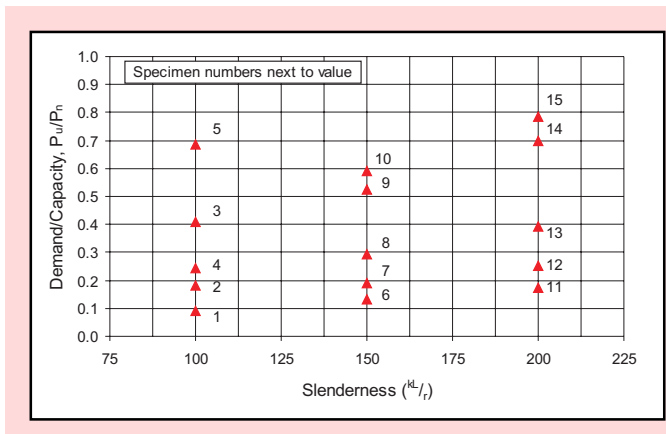
Research Team

*Darren Vian, Graduate
Student, Mettupalayam
Sivaselvan, Graduate
Student, Michel Bruneau,
Professor, and Andrei
Reinhorn, Professor,
Department of Civil,
Structural and
Environmental
Engineering, University at
Buffalo*



■ **Figure 1.** Typical Specimen

sions and mass used were varied within each group. Nominal specimen column widths ranged from 2.8 mm (1/8 in) to 9.8 mm (3/8 in). Column heights ranged from 91.7 mm (5.41 in) to 549.9 mm (21.65 in). Individual columns were



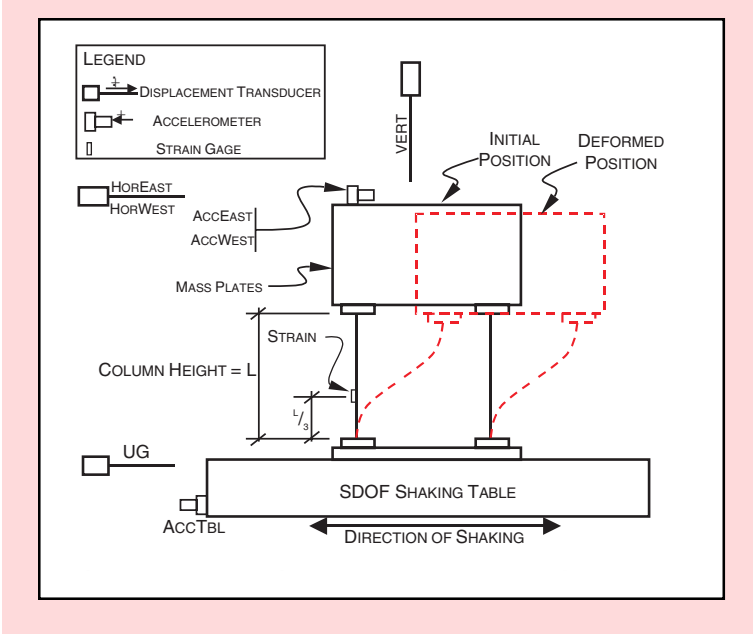
■ **Figure 2.** Specimen Axial Load-to-Strength Ratio versus Slenderness

cut from hot-rolled steel plate and then milled to size. Mass applied to each specimen column varied from approximately 150 kg to 385 kg. Predicted fundamental period of vibration for the specimens, using nominal dimensions, varied from 0.191 sec up to 1.098 sec considering the P- Δ effect. Note that the specimens were not intended to be scaled models of actual structures; therefore unscaled ground motions were used.

A sample column layout is shown in Figure 1. A range of values for axial capacity versus demand, P_u/P_n , was used for each slenderness ratio, where P_u is the weight of the mass plates used in the test, and P_n is the axial capacity of all columns in the specimen, calculated using the AISC-LRFD specifications (AISC 1993). This range of values is shown in Figure 2. A number of initial imperfections were carefully measured and documented, and movement in the transverse direction was prevented by flexible braces verified to have no impact on behavior in the principal direction, as reported in Vian and Bruneau (2001).

A schematic of the test setup and instrumentation is shown in Figure 3. Some special attachments and modifications to standard displacement transducers were developed (Vian and Bruneau, 2001) to ensure reliable measurements up to and

The experimental data and analytical models from this research can be used by other researchers as a benchmark for comparison. Eventually, the research will enable structural engineers to adequately predict when collapse of a given structure will occur, thus ensuring public safety during strong earthquakes.

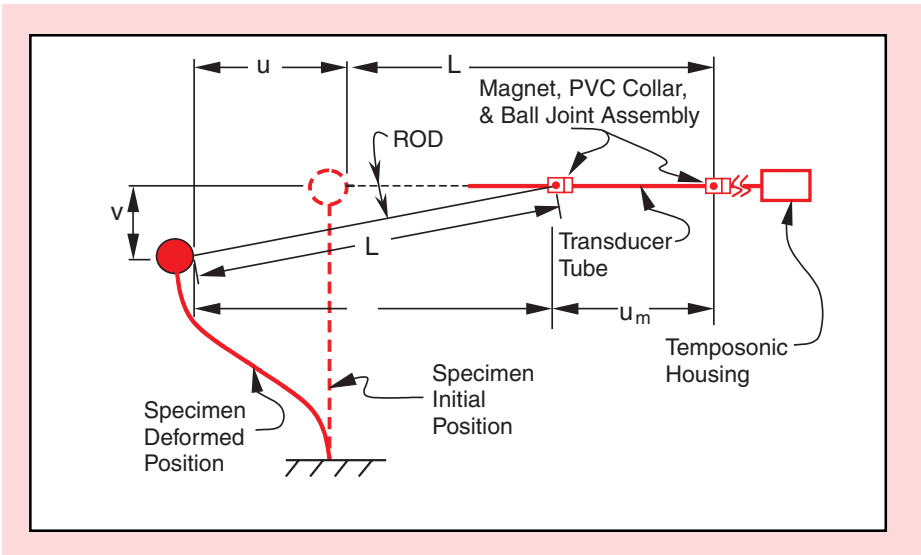


■ **Figure 3.** Schematic of Test Setup and Instrumentation (Looking West)

through collapse, but these details are beyond the scope of this paper.

A free vibration test was first performed on each specimen. Subsequently applied were a number of ground motions progressively increasing in magnitude from approximately two-thirds of the estimated peak elastic response to the esti-

mated peak inelastic response. Among all the data recorded and stored, it is noteworthy that the actual total horizontal displacement of a specimen was calculated using the correction shown in Figure 4.



■ **Figure 4.** Definition of Variables used in Horizontal Displacement

Summary of Test Results

The fundamental period of vibration of each specimen is obtained experimentally via Fourier Spectrum Analysis of the time history data of free-vibration tests. Interestingly, the damping ratio was observed to vary as a function of the amplitude of linear elastic response. Results from the tests to collapse include:

- Seismic response of shake table tests including time history plots of target table acceleration, measured and filtered table acceleration, total mass acceleration, relative mass displacement, as well as a plot of estimated base shear including $P-\Delta$, V_p^* , versus relative displacement.
- Time history plots of relative displacement for each test in the schedule for comparison of displacements throughout the range of progressive collapse.
- Plots of estimated base shear, V_p^* , normalized by the plastic base

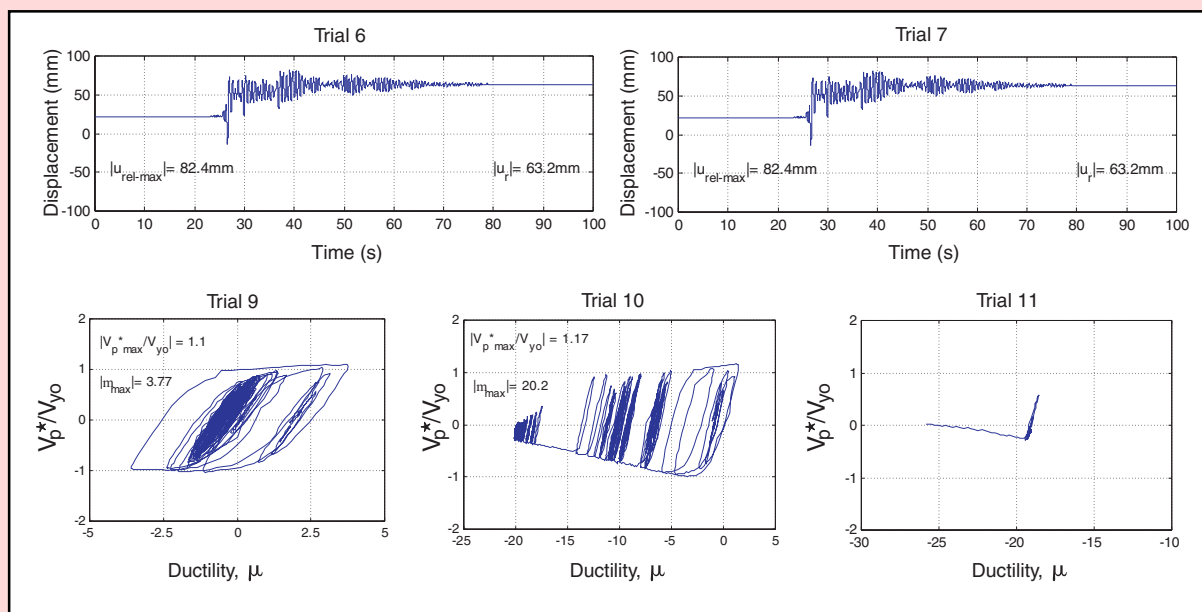
shear, V_{yo} , versus displacement ductility, μ , as well as similar plots of base shear versus percent drift, γ ($=u_{rel-max}/L_{avg}$).

Some typical results are shown in Figure 5.

Behavioral Trends

The value of the stability factor, indicated in the preceding discussion, has a significant effect on the response of the structure. In practical bridge and building structures, θ is unlikely to be greater than 0.10, and is generally less than 0.060 (MacRae et. al., 1993). Specimen 1 is the only one here that has a θ value near that suggested practical range for the stability factor, with a value of 0.065. Specimens 2, 6, and 11 have stability factors slightly larger than the likely upper limit, at 0.123, 0.101, and 0.138, respectively. All other specimens have a value of $\theta \geq 0.155$.

Three dimensionless acceleration parameters were compared with

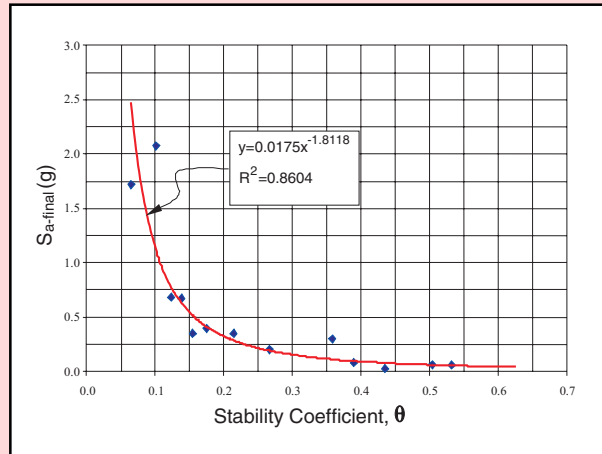


■ Figure 5. Typical Results from Tests to Collapse

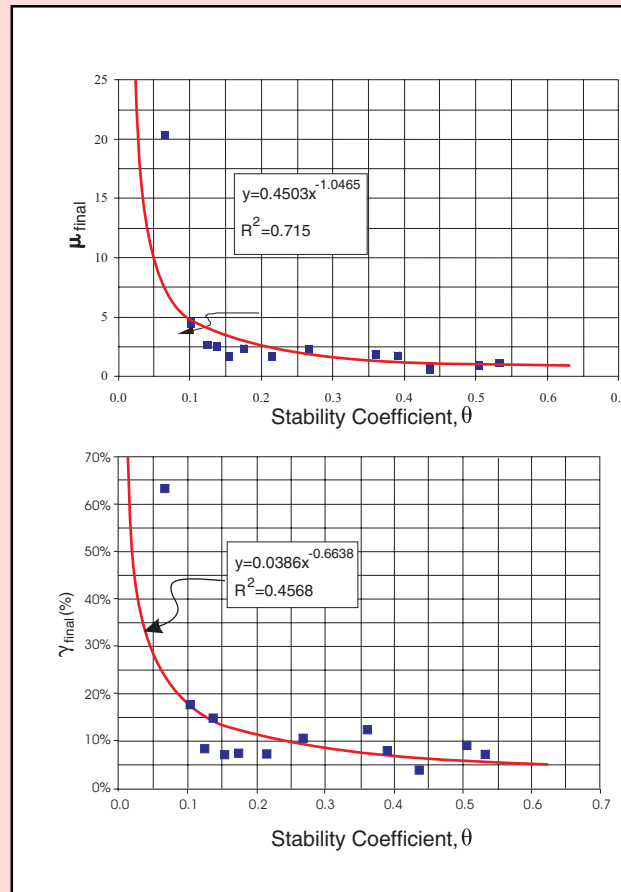
five dimensionless displacement parameters. The following general observations can be made:

- The elastic spectral acceleration, S_a , ductility, μ , and percent drift, γ , were observed to have inverse relationships with θ . In support of this observation, these variables are plotted in Figures 6 and 7 versus the stability factor for the next to last test (given subscript "final"). This suggests that the structures may be less able to undergo large inelastic excursions before imminent instability as the stability factor increases.
- Specimen 1 was the only specimen that underwent both a ductility greater than five (20.35), and a drift larger than 20% of the specimen height (64%), prior to collapse, as shown in Figure 7. Recall that this is the only specimen that has a value of θ less than 0.1.

Overall, these Figures show a high dependence of ultimate inelastic behavior upon the stability factor for a P- Δ affected structure. For the specimens tested in this research, those that had a value of θ equal to or greater than 0.1, tended to have a relatively low level of inelastic behavior before collapse of the structure. Structures with $\theta < 0.1$ were able to withstand ground motions with higher spectral accelerations, experience larger values of ductility, and accumulate larger drifts, than those with $\theta > 0.1$. The more slender structures, characterized by a larger θ value, will undergo relatively small inelastic excursions prior to collapse.



■ Figure 6. Spectral Acceleration versus Stability Coefficient



■ Figure 7. Plots of Displacement Ductility and Drift versus Stability Coefficient

Analytical Modeling and Verification using Data Generated From the Experiments

Data from the experiments performed in this research can be used in the verification of time history analysis programs in the modeling of inelastic structural behavior up to collapse. In these studies, an attempt was made to formulate a flexibility-based planar beam-column element, which can deform inelastically until it loses stability or deteriorates and cannot sustain gravity loads. The formulation has no restrictions on the size of rotations, using one co-rotational frame for the element to represent rigid-body motion, and a set of co-rotational frames attached to the integration points, as customarily used to represent the constitutive equations. The formulation shown in the next section provides an enhancement to the existing models by adding the inelastic behavior in an element, which is stable under static and reversible loads with large deformations using the flex-

ibility approach. The solution procedure associated with the model allows verifying their performance up to complete collapse.

Element Equations

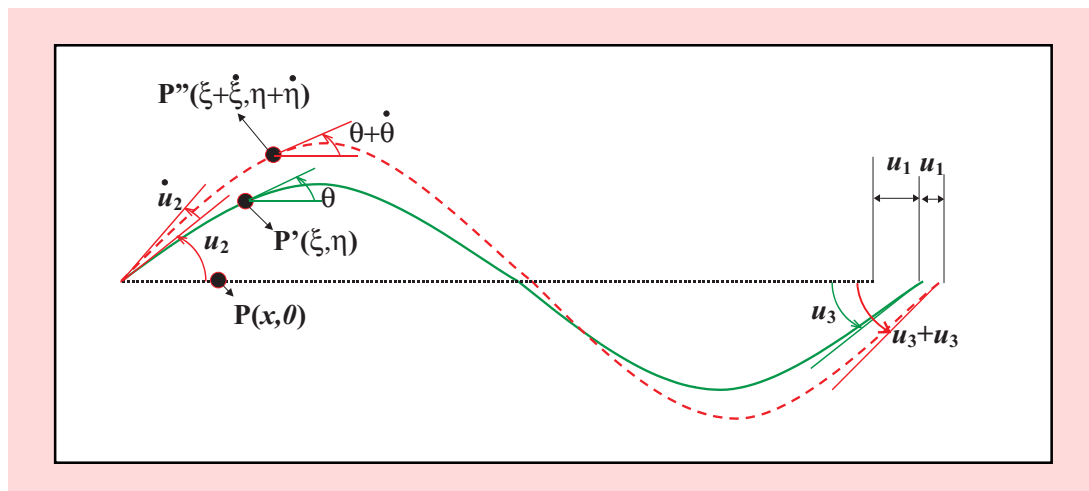
Figure 8 shows the deformed shape of an Euler-Bernoulli beam in co-rotational coordinates attached to the initially straight centerline of the beam. The nonlinear strain displacement relationships are given (Huddleston, 1979) by:

$$\frac{d\theta}{dx} = (1 + \varepsilon)\phi \quad (1)$$

$$\frac{d\xi}{dx} = (1 + \varepsilon)\cos\theta \quad (2)$$

$$\frac{d\eta}{dx} = (1 + \varepsilon)\sin\theta \quad (3)$$

where (ξ, η) is the coordinate of a point which was at $(x, 0)$ before deformation, θ is the angle made by the tangent to the center-line with the horizontal, ε is the axial strain of the centerline and ϕ is the curvature.



■ Figure 8. Euler Bernoulli Beam Subjected to Large Deformation

Considering a small perturbation about this deformed position, the incremental compatibility conditions are given by:

$$\frac{d\dot{\theta}}{dx} = \dot{\varepsilon}\phi + (1 + \varepsilon)\dot{\phi} \quad (4)$$

$$\frac{d\dot{\xi}}{dx} = \dot{\varepsilon} \cos \theta - [(1 + \varepsilon) \sin \theta] \dot{\theta} \quad (5)$$

$$\frac{d\dot{\eta}}{dx} = \dot{\varepsilon} \sin \theta + [(1 + \varepsilon) \cos \theta] \dot{\theta} \quad (6)$$

Integrating these equations over the length of the element and performing a series of integrations by parts, the following variational equation is obtained:

$$\dot{\mathbf{u}} = \begin{Bmatrix} \dot{u}_1 \\ \dot{u}_2 \\ \dot{u}_3 \end{Bmatrix} = \int_0^L \mathbf{b}^T \begin{Bmatrix} \dot{\varepsilon} \\ \dot{\phi} \end{Bmatrix} dx = \int_0^L \mathbf{b}^T \dot{\varepsilon} dx \quad (7)$$

where u_1 = axial displacement, u_2 = rotation at left end and u_3 = rotation at right end as shown in Figure 8, $\tilde{\phi} = (1 + \varepsilon)\phi$ and is found to be the work conjugate of the corotational moment. This agrees with the result of Reissner (1972). \mathbf{b} is a matrix given by:

$$\mathbf{b} = \begin{bmatrix} \cos \theta & -\frac{\sin \theta}{\xi(L)} & -\frac{\sin \theta}{\xi(L)} \\ \eta & \frac{\xi}{\xi(L)} - 1 & \frac{\xi}{\xi(L)} \end{bmatrix} \quad (8)$$

Constitutive Model

In this work, the inelastic behavior of the members is captured in a global sense. The relationships between stress resultants (axial force, bending moment, etc.) and generalized strains (centerline strain, curvature, etc.) are used directly

instead of stress-strain relationships. Simeonov and Reinhorn (2001) derived a smooth three-dimensional plasticity model for arbitrarily shaped yield functions and used it to represent the constitutive behavior of beam-column cross-sections. This model is based on a parallel-spring plasticity model (Park and Reinhorn, 1986, and Nelson and Dorfmann, 1995) with an extension of Bouc-Wen hysteretic model (Wen, 1976, Sivaselvan and Reinhorn, 2000) and its generalization to multiple dimensions by Casciati (1989). The model determines the generalized force, \mathbf{F} , vector (forces and moments) as:

$$\mathbf{F} = \mathbf{F}_e + \mathbf{F}_h \quad (9)$$

$$\mathbf{F}_e = \mathbf{a}\varepsilon \quad (10)$$

$$\dot{\mathbf{F}}_h = (\mathbf{I} - \mathbf{a})\mathbf{K}_0[\mathbf{I} - \mathbf{B}\mathbf{H}_1\mathbf{H}_2]\dot{\varepsilon} \quad (11)$$

where, F_e and F_h are the elastic and hysteretic components of \mathbf{F} , \mathbf{a} is the diagonal matrix of post-yield rigidity ratios, ε is the vector of strains and curvatures, \mathbf{K}_0 is the initial tangent rigidity matrix, \mathbf{I} is the identity matrix and \mathbf{H}_1 and \mathbf{H}_2 , the step functions for yielding and for loading reversals, respectively, are described below. \mathbf{B} is the force-moment interaction matrix:

$$\mathbf{B} = \frac{\left(\frac{\partial \Phi}{\partial \mathbf{F}_h}\right)\left(\frac{\partial \Phi}{\partial \mathbf{F}_h}\right)^T (\mathbf{I} - \mathbf{a})\mathbf{K}_0}{\left(\frac{\partial \Phi}{\partial \mathbf{F}_h}\right)^T (\mathbf{I} - \mathbf{a})\mathbf{K}_0 \left(\frac{\partial \Phi}{\partial \mathbf{F}_h}\right)} \quad (12)$$

where $\Phi(F_p)$ is the yield function. $H_i(F_p)$ is the step function the denoted yielding given by:

$$\mathbf{H}_1 = \left\| \Phi(\mathbf{F}_h) \right\|^N \quad (13)$$

where N is a parameter that governs the smoothness of the transition from the elastic to the plastic state. When N tends to infinity then the model collapses to a bilinear

model. $H_2(F_h, \dot{\epsilon})$ is the step function denoting loading/unloading, given by:

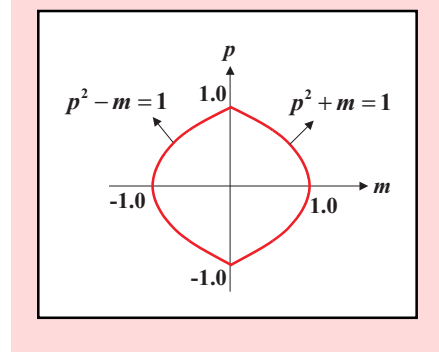
$$H_2 = \eta_1 \operatorname{sgn}(\mathbf{F}_b^T \dot{\epsilon}) + \eta_2 \quad (14)$$

where η_1 and η_2 are parameters that govern the shape of the unloading curve. $\eta_1 + \eta_2 = 1$ to ensure compatibility with classical plasticity theory. It can be noticed that Eq. (7) is an implementation of the principle of virtual forces in rate form.

The compatibility equations (7) and the constitutive equations (9) to (14), are written as a set of differential-algebraic equations (DAE) along with the global equations of motion as proposed by Simeonov et al., (2000). The resulting system of equations is solved by the Backward Difference Method using the routine DASSL (Brenan et al., 1996).



■ Figure 9. Typical Specimen



■ Figure 10. Yield Surface of a Square Cross-section

Verification Study

The results of the above developments are compared to those from other computational solutions as well as with the collapse experiments described above. The parameters of the example for verification were chosen to correspond to specimen 10a (Vian and Bruneau, 2001). This specimen consists of four columns each 137 mm tall and having a square cross-section of side 3.1 mm (see Figure 9). In the first step, the constitutive model of this cross-section is derived. The plastic interaction function of the square cross-section is shown in Figure 10. The yield function for positive and negative directions of the bending moment can be combined to obtain a single yield function as follows:

$$\Phi(P, M) = 2p^2 + m^2 - p^4 - 1 \quad (15)$$

where $p = P/P_p$, $m = M/M_p$, P_p = plastic axial force and M_p = plastic moment.

The formulation for this study is using the yield function and a smoothness parameter $N=2$ in Eq. (13) to represent the transition from initial yield to the plastic state. Equation (15) is substituted in equations (9) to (14) to obtain the necessary constitutive model.

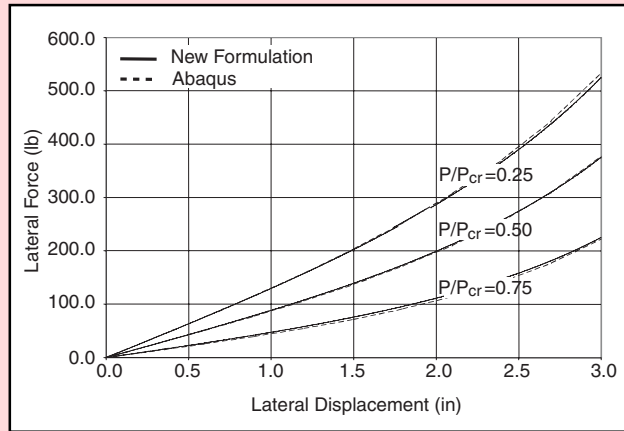
The results obtained from the current formulation and those from the finite element analysis program ABAQUS for monotonic loadings, are shown in Figure 11 with good agreement. Figure 12 shows monotonic deflections of columns leading to complete loss of strength assuming actual elastic material behavior. The slight difference between the results stems from the representation of moment-curvature-behavior in the current approach vs. ABAQUS. The present formulation uses the smoothness parameter $N=2$ to represent the post-yield behavior. While this is sufficient for structural steel sections, a more accurate description is required for a square section. Efforts are underway to incorporate the exact moment-curvature equation presented by Stronge and Yu (1993).

In the dynamic analysis, the specimen was subjected to histories used in the experiment without considering the initial state of the model (previously subjected to series of base motions) and the result is shown in Figures 13 and 14.

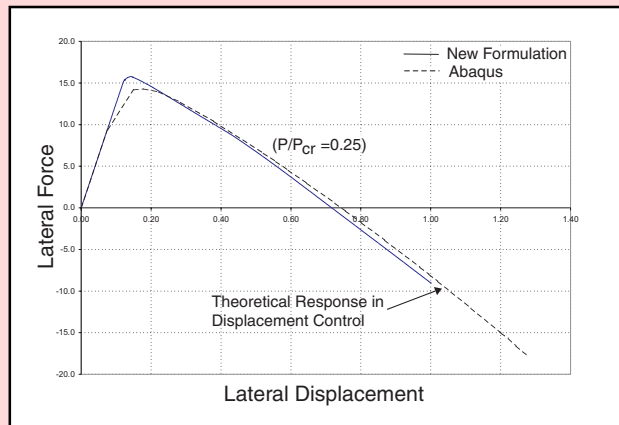
The time history results differ from those obtained in the experiment (see Figure 14). However, when the initial deformation of the model is considered, the analysis model shows same pattern as the experiment as shown in Figure 15.

Comparison with NCHRP 12-49 Proposed $P-\Delta$ Limits

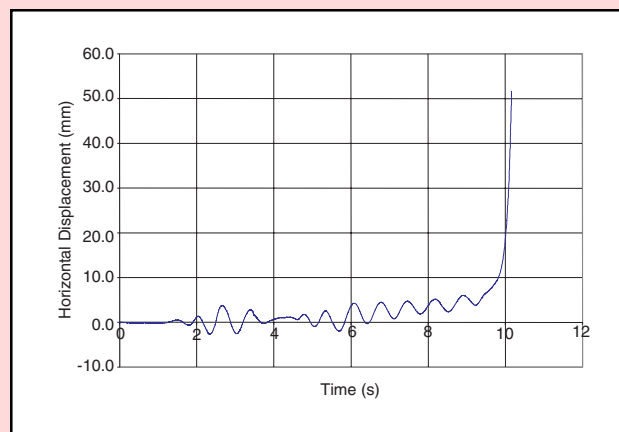
The National Cooperative Highway Research Program (NCHRP), Project 12-49, under the auspices of the Transportation Research Board, is investigating seismic design of bridges from all relevant aspects. At the conclusion of this



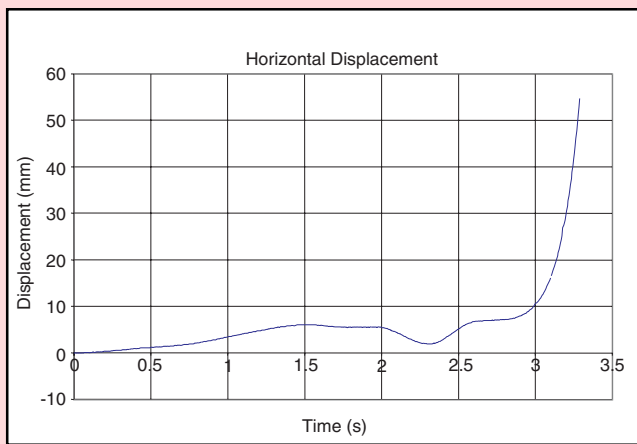
■ Figure 11. Analytical Results for Linear Elastic Material



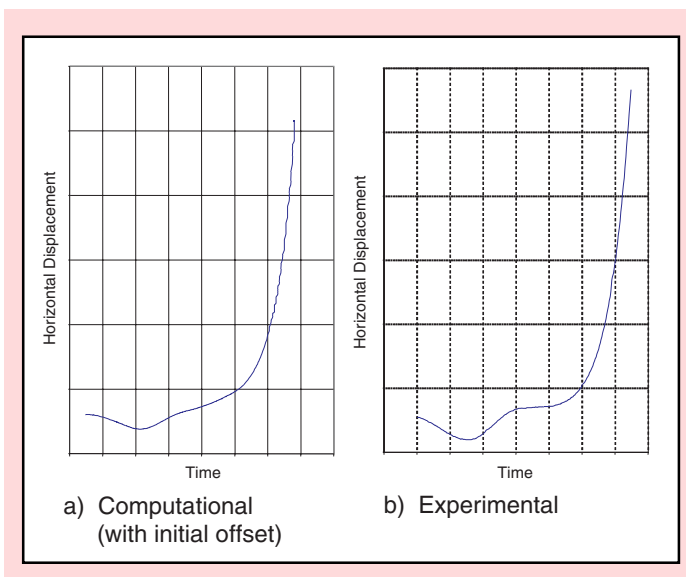
■ Figure 12. Static Analysis with Nonlinear Material



■ Figure 13. Horizontal Displacement from Dynamic Analysis



■ Figure 14. Displacement History from Experiment



■ Figure 15. Displacement Response at the Verge of Collapse

project, proposed revisions to the current LRFD specifications for highway bridges will be presented to the American Association of State Highway Transportation Organizations (AASHTO) for review and possible implementation. Included in the proposed revisions are how additional demands from P- Δ affect structural performance. The most recent proposed provision, as of this writing, states:

The displacement of a pier or bent in the longitudinal and transverse direction must satisfy proposed AASHTO LRFD Equation 3.10.3.9.4-1:

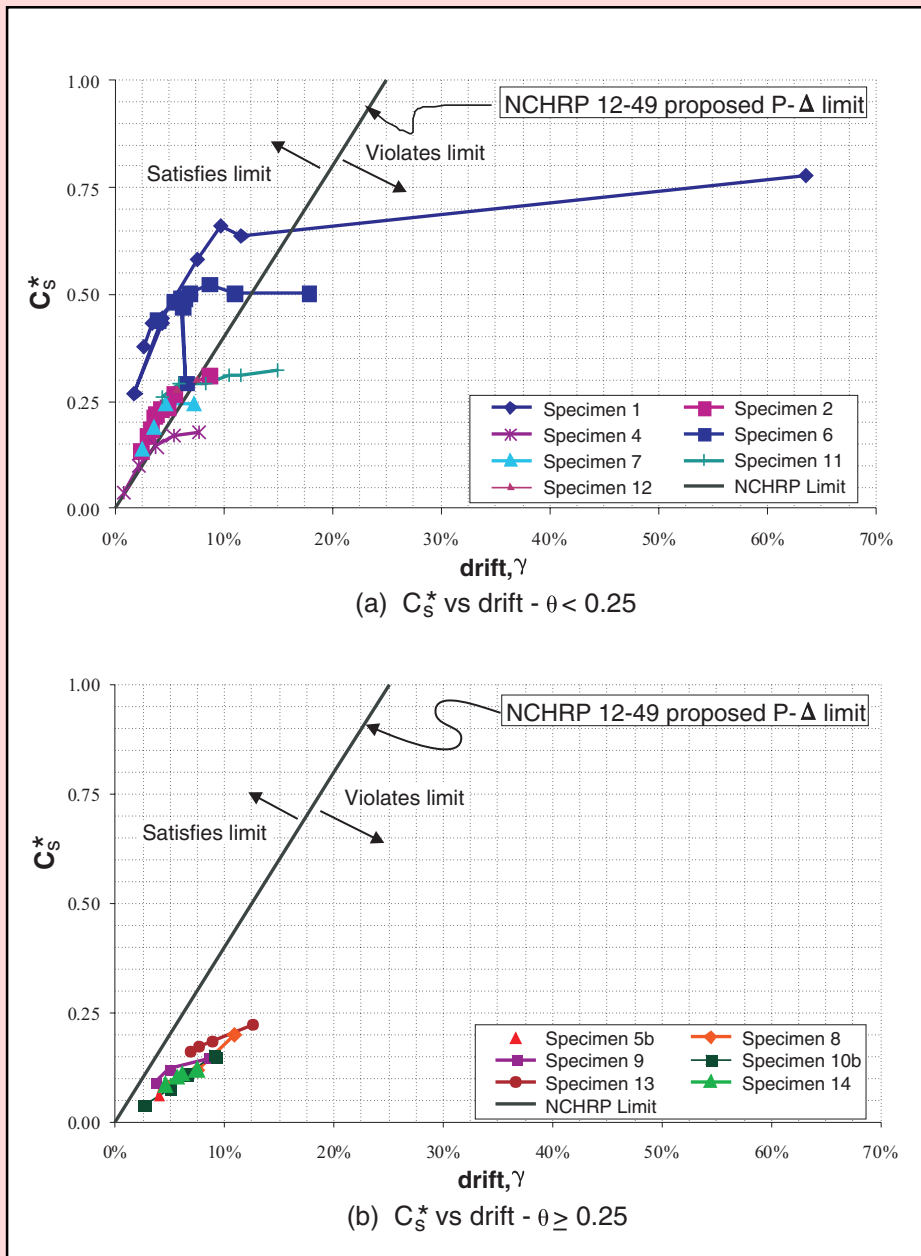
$$\Delta_m \leq 0.25 \cdot C \cdot \left(\frac{W}{P} \right) \cdot H \quad (16)$$

where:

$\Delta_m = R_d \Delta$; R_d is the factor related to response modification factor and fundamental period; Δ is the displacement demand from the seismic analysis; C is the seismic base shear coefficient based on lateral strength; W is the weight of the mass participating in the response of the pier; P is the vertical load on the pier from non-seismic loads; and H is the height of the pier.

For analysis of the specimens in this research, the W/P ratio is equal to unity, and the measured experimental displacements, u_{rel} , and estimated base shear coefficient, C_s^* , can substitute for Δ_m and C , respectively.

Figure 16 compares the proposed limit with the peak experimental responses. The estimated base shear coefficient, C_s^* , is plotted as a function of the maximum drift, γ . Results for specimens with $\theta < 0.25$ (1, 2, 4, 6, 7, 11, and 12) are shown. During the initial tests, when the proposed limit was satisfied, none of these specimens failed. Due to repeated inelastic action, the cumulative drifts of the structure increased, eventually causing progressive collapse and violating the proposed limit. Collapse always occurred only after the limit was exceeded in a prior test, thus validating the proposed criterion. As shown in Figure 16, the remaining specimens, for which $\theta \geq 0.25$, never satisfied the drift criteria, even for those tests that remained



■ Figure 16. Test Results Comparison with NCHRP 12-49 Limits

in the elastic range. The stability factor for these specimens, however, is well above the practical range discussed previously; therefore, the limit violation is of no consequence.

Conclusions

The experimental data generated by this project provides a well-documented database of shake table tests of a SDOF system subjected to earthquakes of progres-

sively increasing intensity up to collapse due to instability. This data will be useful for, and shared with, other researchers who may wish to validate or develop algorithms capable of modeling inelastic behavior of steel frame structures up to and including collapse. The data presented here will also be located on the Internet (with all intermediate data files) for immediate access by other researchers.

An attempt was made to analytically model the collapse using an advanced flexibility based formulation with large deformation inelastic behavior. The verifications and the refinement of the model are done using the experimental data. Parametric studies can be performed with the model to support further codes and standards development efforts.

The research presented here demonstrated a number of impor-

tant points that must be considered in the design of slender steel structures. The stability coefficient, θ , has the most significant effect on the behavior of the structure. As θ increases, the maximum attainable ductility, sustainable drift, and spectral acceleration, which can be resisted before collapse, all decrease. When this factor is larger than 0.1, the ultimate values of the maximum spectral acceleration, displacement ductility, and drift reached before collapse are all grouped below values of 0.75 g, 5, and 20%, respectively. Stability coefficient values less than 0.1 tend to increase each of those response values significantly. The research performed here helped develop a better understanding of the collapse mechanism and provides the tools for further work to modify or improve current design standards.

References

- AISC, (1993), Load and Resistance Factor Design Specification for Structural Steel Buildings, American Institute of Steel Construction, Chicago, IL, December 1.
- Brenan, K. E., Campbell, S.L., and Petzold, L. R., (1996), *Numerical Solution of Initial-value Problems in Differential-Algebraic Equations*, Philadelphia, Society for Industrial and Applied Mathematics.
- Casciati, E., (1989), "Stochastic Dynamics of Hysteretic Media," *Structural Safety*, Vol. 6, No. 2-4, pp. 259-269.
- Huddleston, J. V., (1979), "Nonlinear Analysis of Elastically Constrained Tie-Rods under Transverse Loads," *International Journal of Mechanical Sciences*, Vol. 21, No. 10, pp. 623-630.
- MacRae, G. A., Priestley, M.J.N., Tao, J., (1993), *P- Δ Effects in Seismic Design*, Report No. SSRP-93/05, Department of Applied Mechanics and Engineering Sciences, University of California, San Diego.
- Nelson, R. B. and A. Dorfmann, (1995), "Parallel Elastoplastic Models of Inelastic Material Behavior," *Journal of Engineering Mechanics*, Vol. 121, No.10, pp. 1089-1097.
- Park, Y.J. and Reinhorn, A.M., (1986), "Earthquake Responses on Multistory Buildings Under Stochastic Biaxial Ground Motions," *Proceedings of the Third U.S. Conference on Earthquake Engineering*, Charleston, South Carolina, Vol. 2, pp. 991-1001, August 1986.

References (Cont'd)

- Reissner, E., (1972). "On One-Dimensional Finite-Strain Beam Theory: the Plane Problem," *Journal of Applied Mathematics and Physics (ZAMP)*, Vol. 23, No. 5, pp. 795-804.
- Simeonov, V. K., (1999). *Three-Dimensional Inelastic Dynamic Structural Analysis of Frame Systems*, Ph.D. Dissertation, Civil, Structural and Environmental Engineering, University at Buffalo.
- Simeonov, V. K., Sivaselvan and A. M. Reinhorn, (2000), "Nonlinear Analysis of Structural Frame Systems by the State-Space Approach," *Computer-Aided Civil & Infrastructure Engineering*, Vol. 15, No. 2, pp. 76-89.
- Simeonov, V. K. and Reinhorn, A.M., (2001), *Three-Dimensional Inelastic Dynamic Structural Analysis of Frame Systems*, Technical Report MCEER-01-xx, Multidisciplinary Center for Earthquake Engineering Research, University at Buffalo (in review).
- Sivaselvan, M. V. and Reinhorn, A.M., (2000), "Hysteretic Models for Deteriorating Inelastic Structures," *Journal of Engineering Mechanics*, Vol. 126, No. 6, pp. 633-640.
- Stronge, W. J. and Yu, T.X., (1993), *Dynamic Models for Structural Plasticity*, London, New York, Springer-Verlag.
- Vian, D. and Bruneau, M., (2001), *Experimental Investigation Of P-Delta Effects To Collapse During Earthquakes*, Technical Report MCEER-01-0001, Multidisciplinary Center for Earthquake Engineering Research, University at Buffalo.
- Wen, Y. K., (1976), "Methods of Random Vibration of Hysteretic Systems," *Journal of the Engineering Mechanics Division*, Vol. 102, No. 2, pp. 249-263.

